Electronic Supplementary Material (ESI) for Journal of Materials Chemistry A.

Experimental Details

Preparation of $Ti_3C_2T_x$ (MXene) Nanosheets: LiF (0.99 g) was added to 12M HCl (10 mL), and stirred for 5 min for complete dissolution. To this solution Ti_3AlC_2 (1 g) was added slowly in a course of 10 min to avoid overheating. The reaction mixture was kept at 35 °C for 24 h under magnetic stirring, washed with deionized water and centrifuged, and the supernatant was discarded. These procedures were repeated until the pH value of the supernatant was ~6. The solid was vacuum-filtered by a PTFE membrane, and vacuum-dried. The obtained $Ti_3C_2T_x$ powder was then added to deionized water at a concentration of 1 mg mL^{-1}, and sonicated under argon protection for 1 h to obtain an aqueous solution.[1]

Preparation of BP QDs: Bulk BP (50 mg), synthesized from red phosphorus by heating to 800 °C at 4 GPa for 10 min,[2] was added to NMP (10 mL), and ground for 20 min. NMP (30 mL) was added to this mixture, which was subjected to 300 W sonication for 12 h under argon protection. After sonication, the obtained dispersion was centrifuged at 7000 rpm for 20 min. The top 2/3 supernatant containing BP QDs was collected, and re-centrifuged at 15000 rpm for 20 min. The precipitate was collected and re-dispersed in THF.[3]

Preparation of 2D MXene-Supported BP QDs: Excess BP QDs and MXene nanosheets were mixed in THF, and the mixture was subjected to gentle sonication for 8 h under argon protection. During this process, the BP QDs were spontaneously assembled on the MXene nanosheets by van der Waals attraction. After sonication, the mixture was centrifuged and washed by THF several times. The solid was dried in vacuum, and stored in a glove box filled with argon.

Electrocatalytic HER/OER Tests: The electrocatalyst ink was prepared prior to the electrocatalytic tests. Typically, the electrocatalyst (2.0 mg) was dispersed in 5 wt% Nafion solution (500 μL). A black, uniform ink was formed after sonication for 0.5 h. Then, the ink (7 μL) was slowly pipetted onto a glassy

carbon electrode (GCE) with a surface of 0.07065 cm^2. After drying, a homogeneous layer was fixed on the surface of the GCE. The loading of electrocatalyst was about 0.39 mg cm^{-2}. The Pt/C and RuO_2 electrocatalysts were also loaded on the GCE for HER and OER tests, respectively.

The electrocatalytic performance of the samples was measured in 1.0M KOH solution using a three-electrode mode on an electrochemical workstation (CHI 660D, CH Instruments). A GCE, a graphite rod and a saturated calomel electrode (SCE) were used as the working electrode, counter electrode and reference electrode, respectively. All the potentials were converted to the reversible hydrogen electrode (RHE) based on the equation E(*vs.* RHE) = E(*vs.* SCE) + 0.244 + 0.059 × PH. Before the LSV measurements, the samples were electrochemically preconditioned by cyclic voltammetry (CV) at a scan rate of 50 mV s^{-1} until stable CV curves were obtained. The electrocatalytic performance of the samples was investigated by LSV at a scan rate of 5 mV s^{-1}, and the LSV data were made with 100% ohmic drop (iR) correction. Electrochemical impedance spectroscopy (EIS) was performed by applying an AC voltage of 5 mV from 100 kHz to 0.01 Hz. The electrochemical active surface area (EASA) was measured by the CV scanning method. The scan rates were from 20 to 100 mV s^{-1}, and the measurements were carried out in a potential range where no faradic processes were observed. For the overall water splitting, a two-electrode system, with the BP QDs/MXene nanohybrids as both cathode and anode, was employed. The durability tests were performed by using chronopotentiometric and chronoamperometric measurements.

Characterizations: TEM was performed by a Hitachi HT7700 microscope operated at an accelerating voltage of 100 kV. HRTEM was performed by a JEOL JEM-2010 microscope operated at an accelerating voltage of 120 kV. AFM was performed by a Shimadzu SPM 9700 microscope in the tapping mode. Raman spectroscopy was recorded by a LabRAM HR Evolution spectrometer (λ = 532 nm). XRD was performed by a Bruker D8 Advanced X-ray diffractometer with Cu Kα radiation (λ = 0.154 nm). XPS was performed by a Thermo-Scientific K-Alpha spectrometer.

Computational Details: The Projector Augmented-Wave (PAW) technique was used during the calculations, and the plane-wave energy cut-off was set to 500 eV.[4] Perdew-Burke-Ernzerhof (PBE) functional was applied to treat the correlation-exchange energies of all systems.[5] For BP and $Ti_3C_2T_x$ (MXene) surfaces, the sampling over Brillouin zone was treated by a (3×3×1) Monkhorst-Pack grid, while a (3×1×1) grid was applied to the QDs/MXene nanohybrids. During the geometry optimization process, the total energy tolerance was set to 10^{-5} eV and the force on the atoms was less than 0.03 eV $Å^{-1}$. Furthermore, slab models were used to describe the relevant surfaces and nanohybrids, and a 15 Å vacuum slab was added to all slabs to avoid the pseudo interactions between the periodic images along *z* axis.

To evaluate the HER performance of different electrocatalysts, the Gibbs adsorption energy of a single H atom on different surfaces ($|\Delta G_{H^*}|$) was calculated by the following equation:[6]

$$\Delta G_{H^*} = \Delta E_{H^*} + \Delta E_{ZPE} - T\Delta S \qquad (1)$$

where ΔE_{H^*} was the adsorption energy of H species. ΔE_{ZPE} and $T\Delta S$ were the changes of zero-point energy (ZPE) and entropy (S), respectively. T represented the temperature of the systems and was set to be 298.15 K in the present work. According to the previous report,[6] ΔE_{ZPE} and ΔS could be calculated by:

$$\Delta E_{ZPE} = \Delta E_{ZPE-H^*} - 1/2 E_{ZPE-H_2} \qquad (2)$$

$$\Delta S = S_{H^*} - 1/2 S_{H_2} \qquad (3)$$

It was reported that the contribution from ZPE and S was very close to 0.24 eV.[7] Therefore, based on the above corrections, the Gibbs free energy diagram could be constructed, as depicted in **Figure 5**. Furthermore, to describe the activation characteristic of H_2O molecules on different surfaces, the adsorption energies were calculated by:

$$E_{ad.} = E_{catal.+H_2O} - E_{catal.} - E_{H_2O} \qquad (4)$$

Supporting Figures

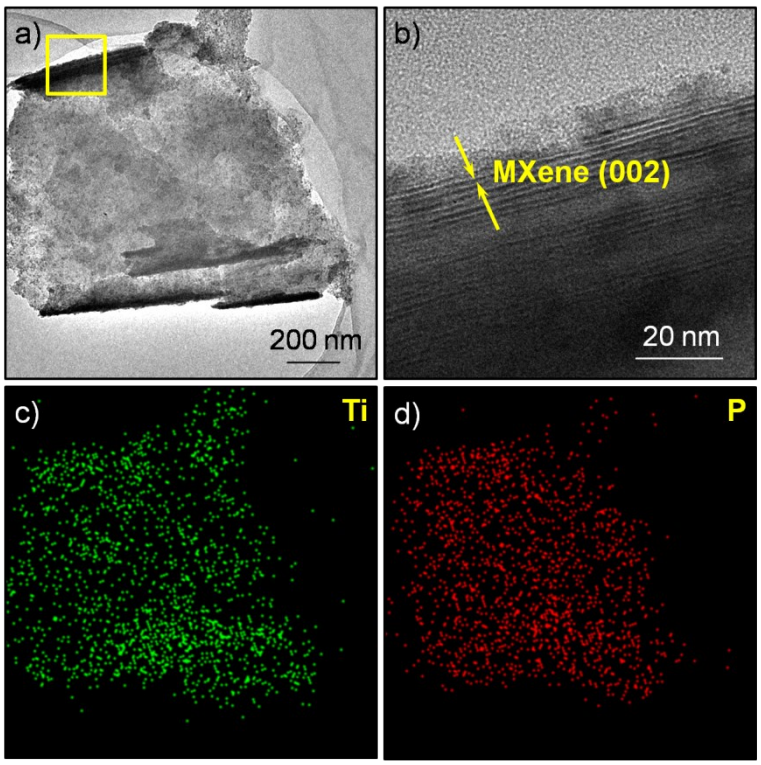

Figure S1. (a) TEM and (b) HRTEM images of BP QDs/MXene nanohybrids, and the corresponding elemental maps of (c) Ti and (d) P.

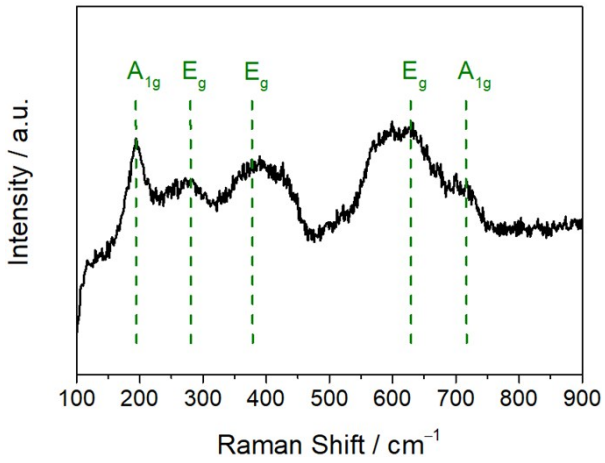

Figure S2. Raman spectrum of $Ti_3C_2T_x$ (MXene), in which the two characteristic bands located at 193 and 716 cm^{-1} result from the out-of-plane A_{1g} vibrations of Ti and C atoms, respectively; and the three characteristic bands located at 282, 370 and 628 cm^{-1} originate from the in-plane E_g vibrations of Ti, C and surface functional groups, respectively.[8] Note that there are no TiO_2 signals in the Raman spectrum, demonstrating our MXene nanosheets were well protected against oxidation during synthesis and assembly.[9]

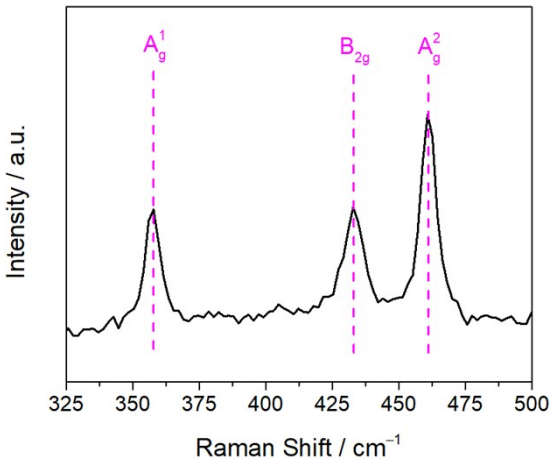

Figure S3. Raman spectrum of BP QDs.

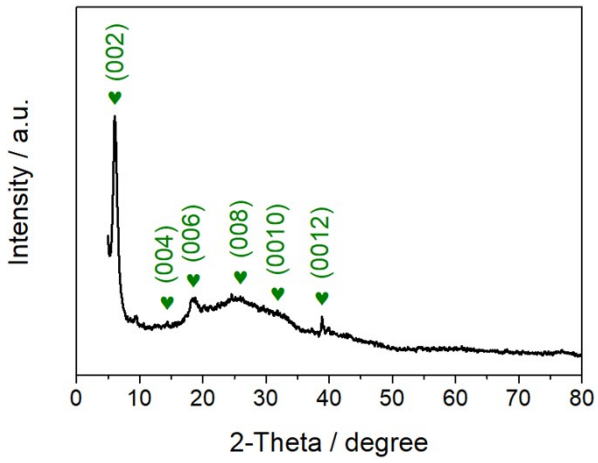

Figure S4. XRD pattern of $Ti_3C_2T_x$ (MXene).

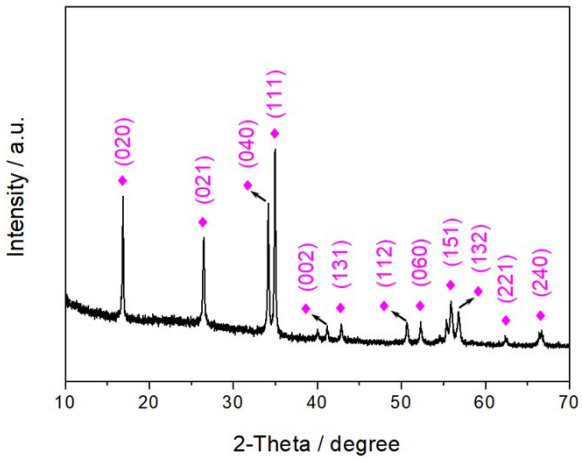

Figure S5. XRD pattern of BP QDs (JCPDS card No. 73–1358).

Table S1. Elemental composition of BP QDs/MXene nanohybrids based on wide-scan XPS survey.

	Ti	C	F	O	P
At%	19.4	11.8	10.8	13.3	44.7
Wt%	32.3	4.9	7.1	7.4	48.2

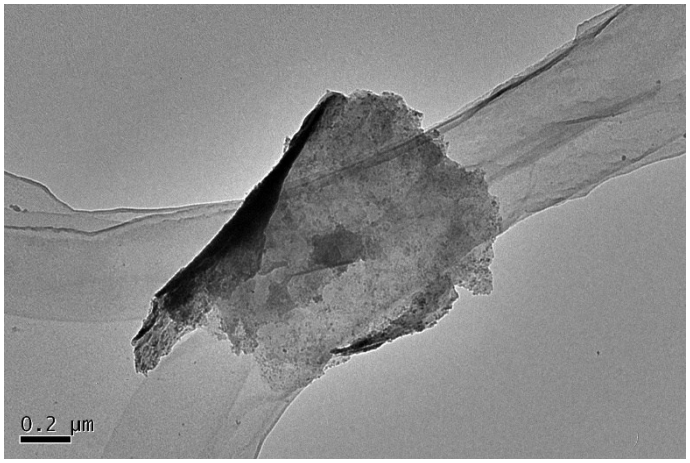

Figure S6. TEM image of BP QDs/MXene nanohybrids after 8 h durability tests (OER).

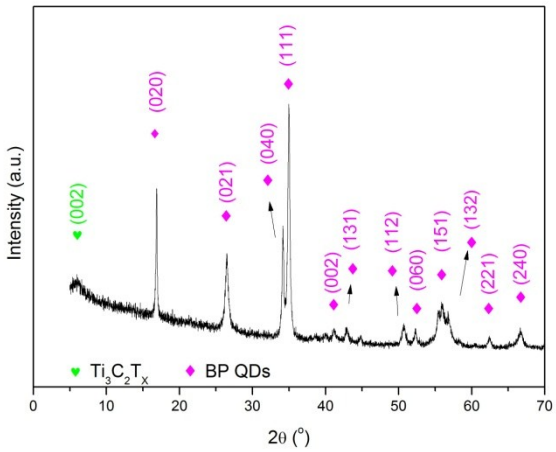

Figure S7. XRD pattern of BP QDs/MXene nanohybrids after 8 h durability tests (OER).

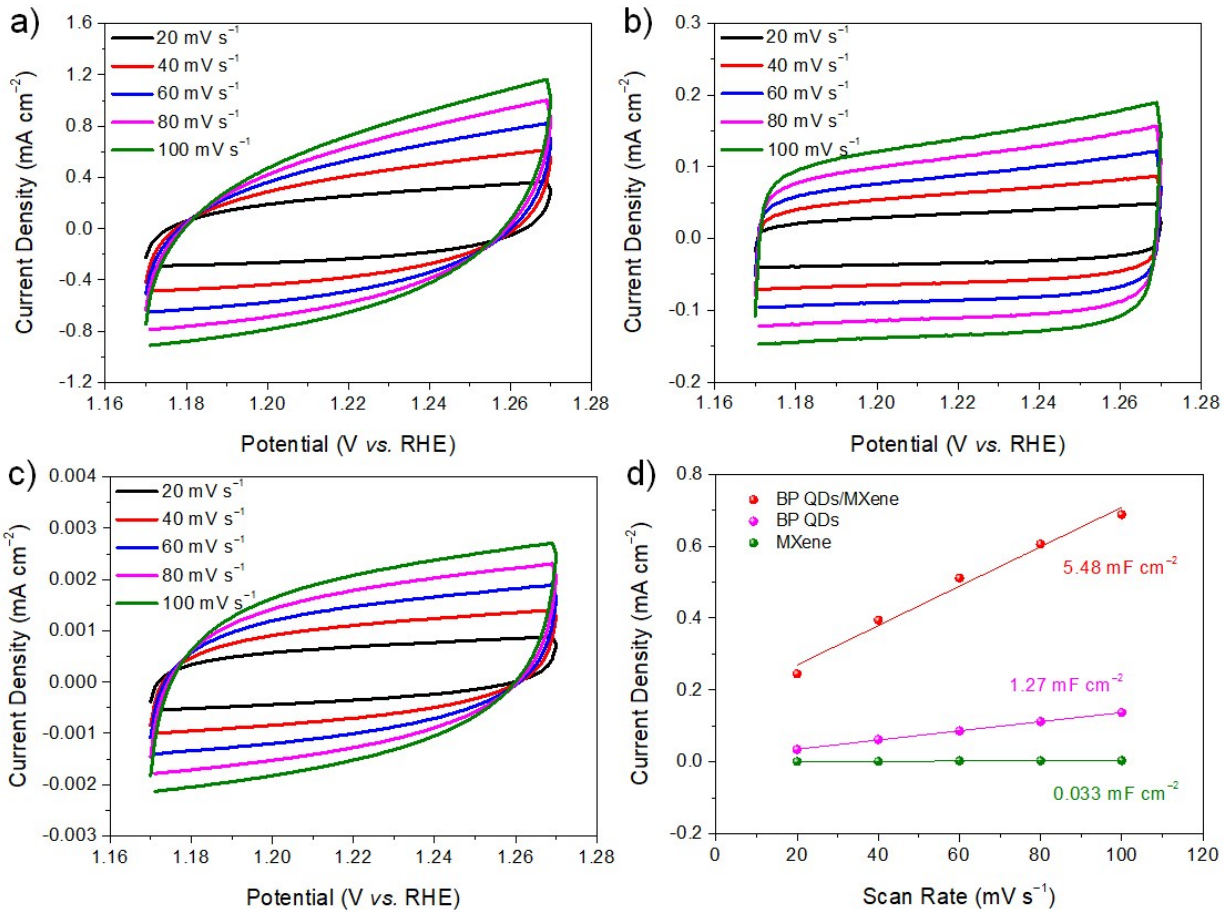

Figure S8. EDLC curves at various scan rates of (a) BP QDs/MXene nanohybrids, (b) BP QDs and (c) MXene nanosheets, and (d) their plots of current density (at 1.22 V *vs.* RHE) *vs.* scan rate for OER.

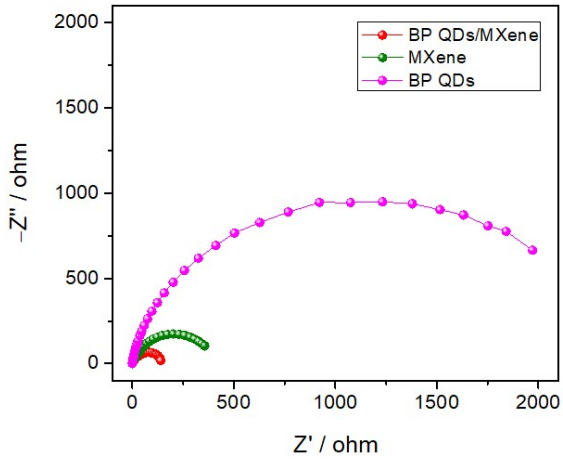

Figure S9. Nyquist plots of BP QDs/MXene nanohybrids, MXene nanosheets and BP QDs.

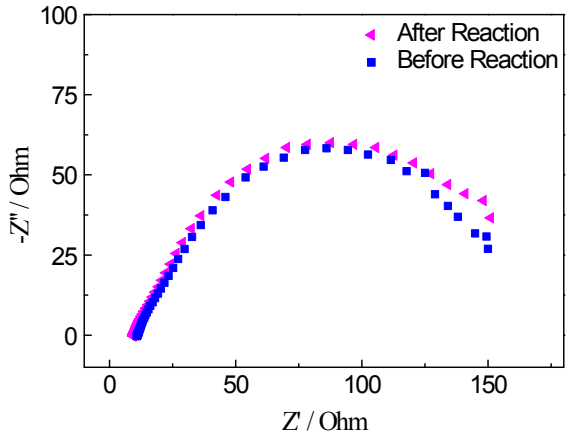

Figure S10. Nyquist plots of BP QDs/MXene nanohybrids before and after 8 h durability test (OER).

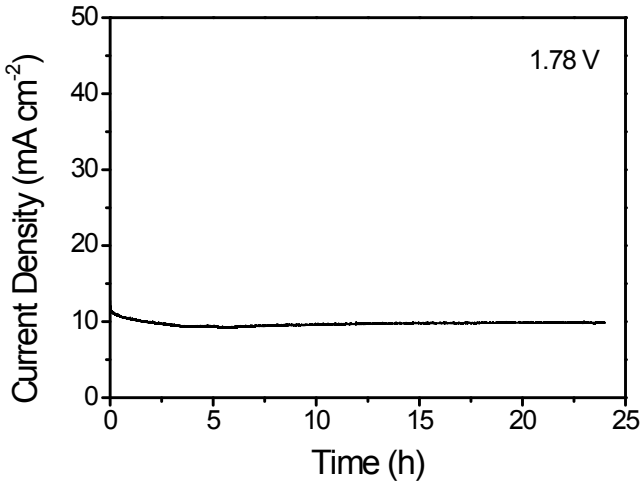

Figure S11. Long-term durability of BP QDs/MXene nanohybrids after overall water splitting.

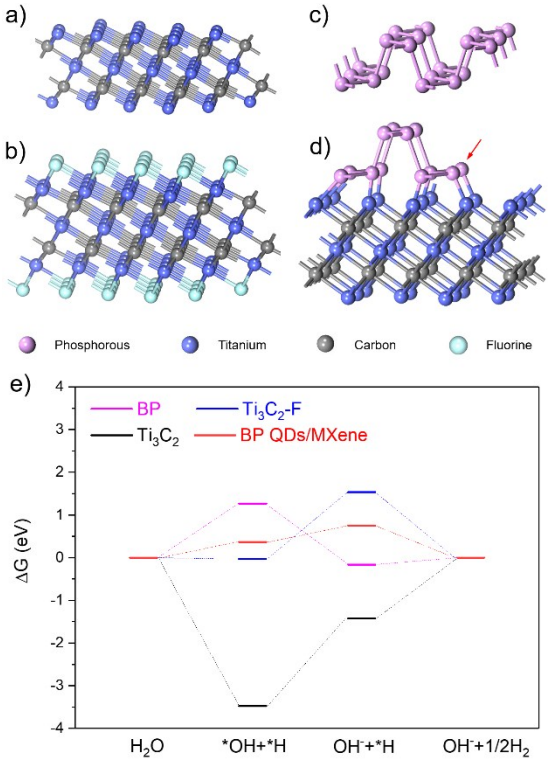

Figure S12. Computational models for (a) pure MXene (Ti_3C_2), (b) F-saturated MXene (Ti_3C_2-F), (c) BP and (d) BP QDs/MXene, and (e) HER activities of these systems in alkaline media (PH = 14). It was reported that the HER process in alkaline media can be described by 3 steps, *i.e.*, water dissociation for generating H* intermediates (Volmer step), desorption of *OH intermediates from catalyst surface, and generation of H_2 (Heyrovsky step).[10] For Ti_3C_2, the Volmer step to form *OH and *H on the catalyst surface (–3.471 eV) is energetically favorable. However, due to the strong interaction between *OH and surface, the desorption of *OH (2.336 eV) is rather difficult, which makes it become the rate-determining step and also suppresses the subsequent process. When Ti_3C_2 surface was saturated by F species, the barrier for water dissociation is very close to zero (–0.031 eV). Although the desorption of *OH from Ti_3C_2-F surface is much easier with respect to Ti_3C_2, the barrier (1.577 eV) remains high. For BP, the energy required for the Volmer step is calculated to be 1.269 eV. As a result, Ti_3C_2, Ti_3C_2-F and BP exhibit poor HER activities. However, when BP is attached to MXene to form nanohybrids, the barriers of the first two steps (0.363 and 0.394 eV) are reduced significantly. As a result, a moderate adsorption–desorption characteristic, which is beneficial to facilitate the overall HER kinetics, is confirmed, and the BP QDs/MXene nanohybrids exhibit an excellent HER activity.

Table S2. Parameters for H_2O molecules adsorbed on different surfaces.

	$E_{ad.}$ (eV)	OH1 Bond (Å)	OH2 Bond (Å)	∠H1OH2 (°)
H_2O[11]	—	0.95720	0.95720	104.5000
BP QDs	–0.192	0.97282	0.97698	104.4387
$Ti_3C_2T_x$ (MXene)	–0.980	0.98773	0.99816	110.0776
BP QDs/MXene	–1.014	0.98497	1.01703	108.6433

Supporting References

[1] a) S. Kajiyama, L. Szabova, K. Sodeyama, H. Iinuma, R. Morita, K. Gotoh, Y. Tateyama, M. Okubo and A. Yamada, *ACS Nano*, 2016, **10**, 3334; b) M.-Q. Zhao, M. Torelli, C. E. Ren, M. Ghidiu, Z. Ling, B. Anasori, M. W. Barsoum and Y. Gogotsi, *Nano Energy*, 2016, **30**, 603.

[2] L.-Q. Sun, M.-J. Li, K. Sun, S.-H. Yu, R.-S. Wang and H.-M. Xie, *J. Phys. Chem. C*, 2012, **116**, 14772.

[3] L. Pan, X.-D. Zhu, K.-N. Sun, Y.-T. Liu, X.-M. Xie and X.-Y. Ye, *Nano Energy*, 2016, **30**, 347.

[4] P. E. Blöchl, *Phys. Rev. B*, 1994, **50**, 17953.

[5] J. P. Perdew, K. Burke and M. Ernzerhof, *Phys. Rev. Lett.*, 1996, **77**, 3865.

[6] J.-S. Li, Y. Wang, C.-H. Liu, S.-L. Li, Y.-G. Wang, L.-Z. Dong, Z.-H. Dai, Y.-F. Li and Y.-Q. Lan, *Nat. Commun.*, 2016,**7**, 11204.

[7] a) J. K. Nørskov, T. Bligaard, A. Logadottir, J. R. Kitchin, J. G. Chen, S. Pandelov and U. Stimming, *J. Electrochem. Soc.*, 2005, **152**, J23; b) Y. Zheng, Y. Jiao, Y. Zhu, L. H. Li, Y. Han, Y. Chen, A. Du, M. Jaroniec and S. Z. Qiao, *Nat. Commun.*, 2014, **5**, 3783.

[8] a) J. Yan, C. E. Ren, K. Maleski, C. B. Hatter, B. Anasori, P. Urbankowski, A. Sarycheva and Y. Gogotsi, *Adv. Funct. Mater.*, 2017, **27**, 1701264; b) Y. Abate, D. Akinwande, S. Gamage, H. Wang, M. Snure, N. Poudel and S. B. Cronin, *Adv. Mater.*, 2018, **30**, 1704749.

[9] a) M. Naguib, O. Mashtalir, M. R. Lukatskaya, B. Dyatkin, C. Zhang, V. Presser, Y. Gogotsi and M. W. Barsoum, *Chem. Commun.*, 2014, **50**, 7420; b) B. Ahmed, D. H. Anjum, M. N. Hedhili, Y. Gogotsi and H. N. Alshareef, *Nanoscale*, 2016, ***8***, 7580.

[10] Y. Luo, X. Li, X. Cai, X. Zou, F. Kang, H.-M. Cheng and B. Liu, *ACS Nano*, 2018, **12**, 4565.

[11] K. Refson, R. A. Wogelius, D. G. Fraser, M. C. Payne, M. H. Lee and V. Milman, *Phys. Rev. B*, 1995, **52**, 10823.